Analytical Methods

ROYAL SOCIETY OF CHEMISTRY

PAPER

View Article Online
View Journal

Cite this: DOI: 10.1039/d0ay01481h

Sensitive detection of microRNA using QCM biosensors: sandwich hybridization and signal amplification by TiO_2 nanoparticles

Ji Yoon Lim† and Soo Suk Lee †*

MicroRNA-21 (miR-21) is known to act as an important biomarker for cancer, in that its up-regulation is closely related to several types of malignant tumor. Sensitive and accurate detection of miR-21 using a biosensor is highly challenging. In this study, sensitive and selective detection technology for miR-21 molecules using a quartz crystal microbalance (QCM) biosensor was developed. Sandwich hybridization between miR-21 and specially designed probes and a subsequent TiO_2 photocatalytic silver enhancement reaction were the driving forces for sensitive detection with high selectivity for miR-21. Using this strategic approach under optimal conditions, the novel QCM biosensor can detect miR-21 with a LOD of 0.87 pM over the entire linear range from 0.1 pM to 10 μM, with a correlation coefficient of 0.988. In addition, the developed QCM biosensor was very effective in the quantification of miR-21 in serum samples, so the proposed miRNA detection method offers great potential for the diagnosis of early disease, such as cancer and vascular diseases, and could be an excellent alternative for biological research and clinical diagnosis.

Received 4th August 2020
Accepted 5th October 2020

DOI: 10.1039/d0ay01481h

rsc.li/methods

Introduction

Biosensors are defined as analytical devices that detect biological and chemical substances by generating electrical, thermal, or optical signals as the result of specific biochemical reactions. In general, biosensors provide an efficient and rapid method for the detection of biochemical substances, and offer the advantages of small sample volume, simple sample preparation, high selectivity and sensitivity, and miniaturization of the devices.[1] The development of highly sensitive and selective biosensors for the rapid and accurate detection of biomolecular interactions, such as enzyme–substrate reactions, protein–protein interactions, and nucleic acid–nucleic acid hybridization, is one of the most important goals of research in this field. Biosensors have two basic components: a bioreceptor, where a biochemical reaction occurs; and a transducer, which converts the result of the biochemical reaction into a physical signal. Depending on the transducer's signal conversion mechanism, biosensors are classified into optical, electrochemical, piezoelectric, and thermal biosensors.[2] The quartz crystal microbalance (QCM) is one of the most studied typical piezoelectric transducers, and is known to be a very stable and accurate oscillator that can measure nanogram-level mass change per unit area on the sensor surface, through the measuring changes in resonance frequency of a quartz crystal resonator.[3–8] The QCM biosensor also provides a rapid response time, superb detection sensitivity, experimental simplicity, and cost effectiveness, due to its simple structure, allowing the efficient real-time detection of target analytes in biological samples. In the detection of target biomaterials using QCM biosensor, the reproducibility of detection and the improvement of sensitivity are very important from the viewpoint of the early diagnosis of disease, which is also the ultimate goal of all biosensors. Therefore, much effort has been made to explore new approaches to improve detection sensitivity for low-concentration biomolecule analysis, and the most representative method is a signal amplification strategy.[9–14]

Recently, signal enhancements associated with the use of nanoparticle labeling have been widely used for sensitive biomolecule detection.[15–20] Colloidal gold nanoparticles (AuNP) have most widely been used as labeling materials for amplifying analytical signals in biomolecules detection. Titanium dioxide (TiO_2) nanoparticles are also used as labeling materials for signal amplification in the detection of biomolecules.[21–24] When the surface of the TiO_2 nanoparticle, a semiconductor photocatalyst, is exposed to UV light ($\lambda < 384$ nm) having a bandgap energy of 3.23 eV or higher, separation of charges occurs at the particle surface (a positive hole (p^+) in the valance band, and an electron (e^-) in the conduction band) and the electron in the conduction band in the particle can reduce surrounding molecules in the medium.[21] The photocatalytic reduction of silver ions to metallic silver occurs only on the surface of TiO_2 nanoparticles; it is expected that by applying this technique to QCM biosensors, the high-sensitivity detection of various biomaterials will become possible.

The synergic combination of TiO_2 photocatalysis and photocatalytic silver enhancement technology in the application of QCM biosensors for microRNA (miRNA) detection will be very

Department of Pharmaceutical Engineering, Soonchunhyang University, Asan-Si, 31538, Republic of Korea. E-mail: sslee0810@sch.ac.kr

† Equally contributed.

effective in increasing the detection sensitivity. Recently, miRNAs have been the most promising diagnostic and prognostic markers for many basic biomedical research and clinical applications.[25–28] These are endogenous and naturally occurring single-stranded non-coding RNA molecules that are small in size with (21–25) nucleotides. miRNA has been reported to regulate gene expression by binding to a target messenger RNA (mRNA) having a complementary sequence. Therefore, through the analysis of specific miRNA expression patterns, it may be possible to utilize miRNAs as biomarkers for various human diseases, such as cancer, immune disorders, infectious diseases, and vascular diseases.

In the present study, we demonstrate the detection of miR-21 using QCM biosensor with sandwich hybridization and TiO_2 nanoparticle-based photocatalytic signal amplification techniques. miR-21 is expressed specifically in mammalian cells, and its up-regulation is known to be associated with several types of malignant tumors.[29,30] Scheme 1 shows a schematic of the sandwich hybridization reaction and the UV photocatalytic silver enhancement reaction using the target miR-21, DNA capture probe, and DNA detection probe conjugated with TiO_2 nanoparticles. The preparation of a self-assembled monolayer (SAM) of probe DNA on the QCM biosensor surface, and the synthesis of a TiO_2-conjugated DNA probe with partial complementarity to miR-21, were investigated. The quantitative detection of miR-21 using sandwich hybridization reaction and continuous photocatalytic silver enhancement signal amplification was then discussed.

Experimental

Reagents and apparatus

The reagents (3-glycidyloxypropyl)trimethoxysilane (3-GPTMS), TiO_2 (anatase), silver nitrate, and 6-amino-1-hexanol were purchased from Sigma-Aldrich Chemical Co. (St. Louis, MO, USA), and used without further purification. Human serum was obtained from Thermo Fisher Scientific (Eugene, OR, USA). The 20× saline sodium citrate (SSC) buffer was also purchased from Sigma-Aldrich, and diluted with nuclease-free water obtained from Sigma-Aldrich to make 1× solution. SSC buffer 1× contains 150 mM NaCl in 15 mM sodium citrate (pH 7.0). All organic solvents were purchased from Daejung Chemicals & Metals Co., Ltd. (Seoul, South Korea). HPLC purified synthetic miRNAs (miR-21, miR-124 and miR-155) and a 5′-amine modified DNA capture probe and 3′-amine modified DNA detection probe were obtained from Bioneer (Daejeon, Korea) in lyophilized form, and their sequences were as follows: miR-21 (target miRNA), 5′-UAGCUUAUCAGACUGAUG-UUGA-3′; miR-124 (control miRNA-1), 5′-UAAGGCACGCGGUGAAUGCC-3′; miR-145 (control miRNA-2), 5′-UUAAUGCUAAUCGUGAUAGGGGUU-3′; 5′-amine modified DNA capture probe, 5′-$H_2N(CH_2)_6$-TTTTCAACATCAG-3′; 3′-amine modified DNA detection probe, 3′-$H_2N(CH_2)_6$-TTTATCGAATAGT-5′.

A QCM detection system was used to measure the real-time responses occurring at the QCM biosensor surface, such as the hybridization reaction and signal amplification process for miRNA detection. The mass loading effects by miRNA hybridization and subsequent signal amplification process on a silicon dioxide (SiO_2)-coated QCM resonator (9 MHz resonant frequency; 5 mm sensing diameter) are measured by real-time change in resonance frequency by a Princeton Applied Research QCM922A sensor (SEIKO EG & G, Tokyo, Japan). All experiments for miRNA detection were performed under static conditions without an automatic fluid transfer device at room temperature (RT), and about 50 μL of sample was used for each experiment.

Immobilization of capture and DNA detection probes on SiO_2-coated QCM biosensor and TiO_2 nanoparticles

Silicon dioxide (SiO_2)-coated QCM biosensor chip and TiO_2 nanoparticles were sequentially cleaned with deionized water

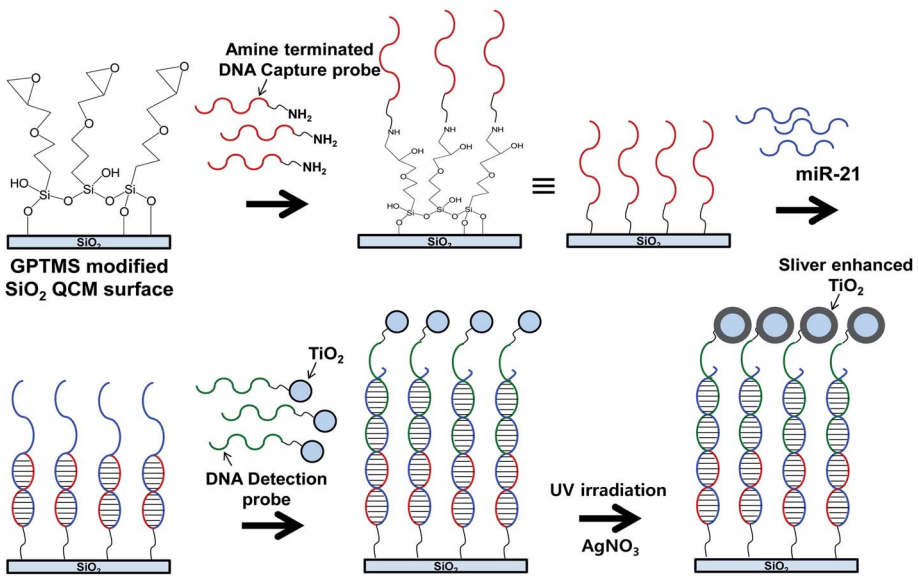

Scheme 1 Schematics of the sandwich hybridization and TiO_2 photocatalytic silver enhancement for the detection of miR-21 using the QCM biosensor. SiO_2 coated QCM biosensor surface was initially treated with (3-glycidyloxypropyl)trimethoxysilane (3-GPTMS).

and methanol, and then dried under a nitrogen atmosphere. They were next activated in a UV-ozone chamber (144AX-220; Jelight Company Inc., Irvine, CA, USA) for 10 min, followed by incubation in 3% (vol/vol) 3-GPTMS in methanol for 1 h. After washing with methanol for 2 min and drying under nitrogen, they were baked at 110 °C for 1 h in the oven, followed by being washed again with methanol, and dried under nitrogen. The 5′-amino-modified DNA capture probe was attached to the surface of the 3-GPTMS-modified QCM biosensor chip, and the 3′-amino-modified detection DNA probe was attached to the surface of the 3-GPTMS-modified TiO_2 nanoparticle, according to the following protocol: the 3-GPTMS-modified QCM biosensor chip and TiO_2 nanoparticle were treated with 25 μM concentrations of 5′-amino-modified DNA capture probe and 3′-amino-modified detection DNA probe dissolved in 100 mM sodium phosphate buffer at pH 8.5, respectively. The excess epoxide groups of 3-GPTMS were deactivated with 50 mM 6-amino-1-hexanol in 100 mM sodium phosphate buffer at pH 8.5 for 30 min at 37 °C. The sensor chip and TiO_2 nanoparticles were washed with sodium phosphate buffer, and finally with doubly distilled water. The capture probe-modified sensor chips were desiccated for storage at RT until use, and the detection probe-modified TiO_2 nanoparticles were stored in nuclease-free water at 4 °C.

Detection of synthetic miR-21 in the QCM sensing system

For the detection of synthetic miR-21 in a 1× SSC buffer solution (pH 7.0) using a QCM biosensor system, various concentrations (0.10 pM to 10 μM) of synthetic miR-21 were first hybridized with DNA capture probe immobilized on a QCM biosensor chip for 30 min at RT. Next, the DNA detection probe conjugated with TiO_2 nanoparticles was introduced to the partially hybridized sensor surface formed above, and allowed to stand for 30 min to form a sandwich hybridization. After washing with SSC buffer solution for 1 min, silver nitrate solution (10 mM) was added to the sensor surface, and irradiated with UV light, using a UV hand lamp with a wavelength of 365 nm (Vilber Lourmat, France) equipped with 4 W UV discharge tubes, to induce silver enhancement reaction by photocatalytic reduction reactions. After 10 min exposure, the QCM sensing surface was then washed again with SSC buffer solution. We carried out the same processes with 10 nM concentration of miR-124 and miR-155 as control experiments. Each experiment was performed in triplicate for all miRNAs, with replicates performed on different days. In addition, we also conducted the same experiments using various concentrations (0.10 pM to 10 μM) of synthetic miR-21 spiked in normal human serum.

Photometric measurement of TiO_2-based photocatalytic silver ion reduction

To prove the TiO_2-based photocatalytic silver deposition, TiO_2 nanoparticles were immersed in $AgNO_3$ aqueous solution. The concentration of silver salt varied from (1.0 to 10) mM. Finally, the solution was exposed to UV radiation for (1–30) min. It then turned a dark color, indicating the presence of silver particles. The UV-VIS absorption spectrum was recorded by BioTek's Epoch 2 microplate spectrophotometry (Winooski, VT, USA) and 96-well plates obtained from Thermo Fisher Scientific (Bremen, Germany). We repeated these experiments thrice.

Results and discussion

Detection principle of miR-21 on QCM biosensor surface

Scheme 1 shows the detection of target miR-21 based upon sandwich hybridization format using a capture probe and a detection probe conjugated with TiO_2 nanoparticles and signal amplification strategies on the QCM biosensor surface, in combination with photocatalytic silver enhancement reaction by UV irradiation. Firstly, a DNA capture probe was covalently immobilized to the 3-GPTMS coated QCM biosensor surface, and then target miR-21 was partially hybridized to the DNA capture probe. Secondly, the sandwich hybridization between the target miR-21 and the complementary two probes was formed after introducing the DNA detection probe with attached TiO_2 nanoparticles. Finally, size enlargement of the TiO_2 nanoparticles by photocatalytic silver enhancement processes will cause amplification of the QCM resonant signal intensity. Thus, the highly sensitive and specific detection of miR-21 can be obtained based on this hybridization and subsequent signal amplification strategy. In this miR-21 detection process, the photocatalytic silver enhancement step is the most important part in improving signal intensities and detection reproducibility. Without signal amplification, the amount of change in the resonance frequency is too small to detect the miR-21 with high sensitivity. Therefore, it is no exaggeration to say that the majority of the total QCM resonance frequency fluctuation is created by this signal amplification process. In this regard, we performed atomic force microscopy (AFM) and transmission electron microscopy (TEM) analysis to confirm the QCM biosensor surface before and after the photocatalytic silver staining reaction based on TiO_2 nanoparticles. Fig. 1(a) and (b) show atomic force microscopy (AFM) images of sandwich hybridization results including TiO_2 nanoparticles on glass slides before and after photocatalytic silver staining processes. For clear AFM images, we analyzed the results of a sandwich hybridization performed using commercial glass slides under the same conditions as on SiO_2-coated QCM biosensors. The 4 μm × 4 μm surfaces were scanned and the brighter spots in Fig. 1(a) are TiO_2 nanoparticles (the circled larger particles are seems to be aggregated forms). The size of the TiO_2 nanoparticles was increased by photocatalytic silver staining after UV irradiation as shown in Fig. 1(b). In addition, Fig. 1(c) and (d) show typical TEM images for bare TiO_2 nanoparticles and the TiO_2/Ag composites, respectively. The latter is a form in which Ag nanoparticles are deposited uniformly on the surface of TiO_2. The deposited Ag nanoparticles appear as dark spots in the TEM image as shown in Fig. 1(d).

Condition optimization

In order to achieve good analytical performance, we optimized the concentration of $AgNO_3$ solution and UV irradiation time for

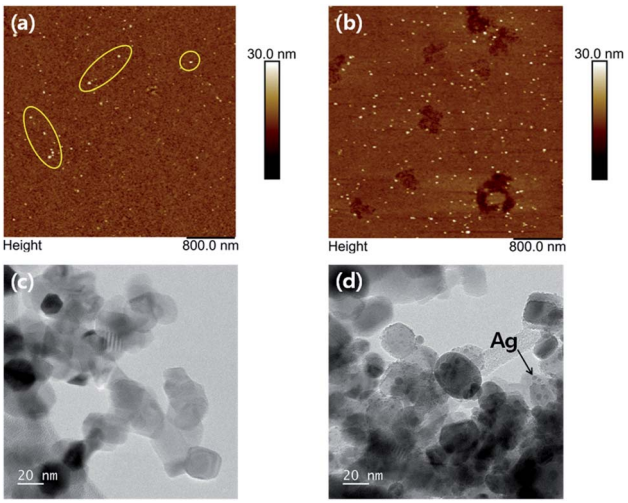

Fig. 1 AFM images of miR-21-DNA duplex hybrid conjugated with TiO_2 nanoparticles (a) before and (b) after photocatalytic silver staining process and TEM images of (c) TiO_2 nanoparticles and (d) TiO_2/Ag composites, respectively.

the photocatalytic silver enhancement conditions that have the greatest effect on signal intensity. Optimization for the UV irradiation time was achieved by adding TiO_2 nanoparticles to 5 mM $AgNO_3$ aqueous solution, and measuring the change in absorbance at 482 nm according to UV irradiation time. On the other hand, the dependence of $AgNO_3$ concentration was investigated through the changes in resonance frequency by TiO_2-induced photocatalytic silver enhancement reaction for 10 min according to the concentration of $AgNO_3$ solution, after the sandwich hybridization process was performed on the QCM biosensor. Fig. 2 shows the change in absorbance at 482 nm by silver deposited on the surface of TiO_2 nanoparticles with photocatalytic silver enhancement as a function of UV exposure time in 5 mM $AgNO_3$ solution. The change in absorbance increased with UV exposure time, followed by saturation after 30 min. We decided on the UV exposure time of 10 min, considering the overall reaction time with this result. On the other hand, the efficiency of the photocatalytic reduction reaction could be improved by increasing the concentration of $AgNO_3$. At this time, the UV power was kept constant, in order to exclude the effect of the UV power on the photocatalytic reduction reaction. Fig. 3 shows the change in resonance frequency according to the concentration of $AgNO_3$ after sandwich hybridization using 1.0 μM synthetic miR-21, and a subsequent photocatalytic reaction for 10 min. The change in resonance frequency increases linearly with $AgNO_3$ concentration. At 10 mM $AgNO_3$ solution, the highest concentration in this experiment, the total frequency change due to sandwich hybridization and photocatalytic silver enhancement was found to be approximately 2.48 kHz. However, with 10 mM $AgNO_3$, the coefficient of variation (% CV) value in three replicates was as high as 38%, so we decided to use the highest concentration of 5 mM with good reproducibility in this study. In fact, as a result of the 10 mM $AgNO_3$ experiment, we observed that the size of silver-deposited TiO_2 nanoparticles increased excessively, while the aggregated nanoparticles detached from the QCM biosensor surface.

Real-time response of QCM sensing for miR-21

Fig. 4 provides the real-time response of the resonance frequency and resonance resistance of the QCM biosensor for miR-21 detection. Overall, the resonance frequency was decreased by an increase in mass as a result of the chemical reactions at the sensor surface; and conversely, the resonance resistance was increased.[31,32] It contained the following three steps: (1) hybridization of the DNA capture probe and miR-21, (2) sandwich hybridization of the DNA capture probe, miR-21, and TiO_2-conjugated DNA detection probe, and (3) size enlargement of the TiO_2 nanoparticles by the photocatalytic silver enhancement processes. As expected, the sandwich hybridization resulted in a substantial decrease in resonance frequency, and increase in resonance resistance. However, the photocatalytic silver enhancement process led to much higher decrease of frequency and increase of resistance. The resonance frequency decreased and the resonance resistance increased

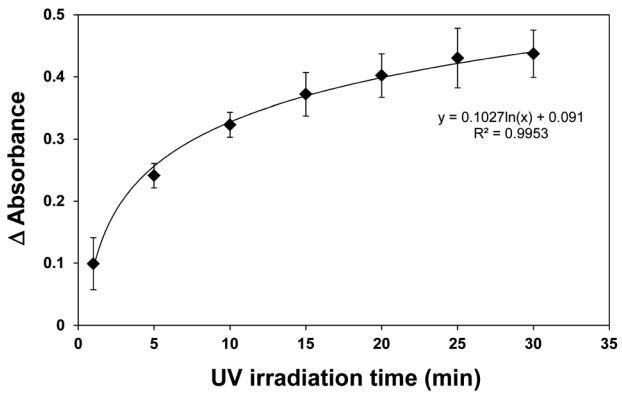

Fig. 2 Variations in the changes in absorbance of TiO_2 aqueous solution as a function of UV (365 nm) irradiation time in a 5 mM $AgNO_3$ solution.

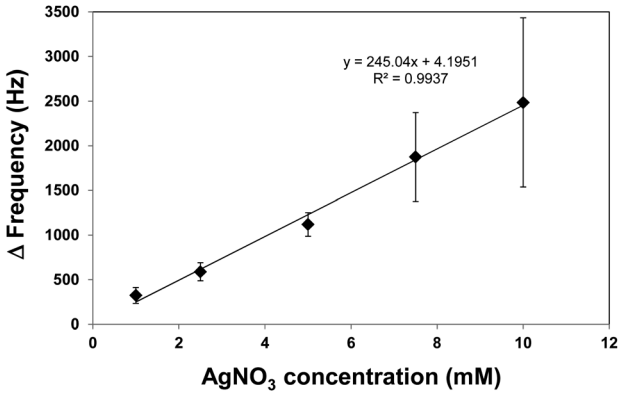

Fig. 3 Variations in the changes in resonance frequency of the results of the miR-21 detection assay including sandwich hybridization, and a subsequent TiO_2 photocatalytic silver enhancement reaction, as a function of $AgNO_3$ concentration, for 10 min UV irradiation.

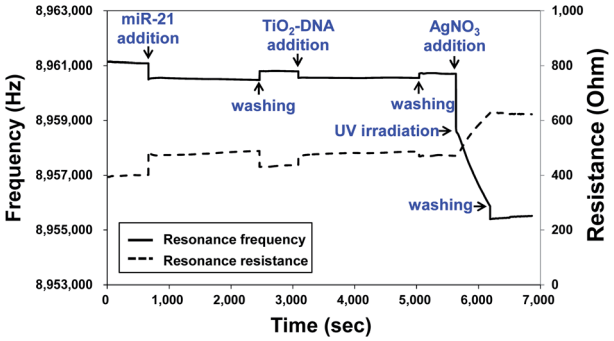

Fig. 4 Difference in change in resonance frequency (solid plot) and resonance resistance (dashed plot) by QCM measurements. In this experiment, 1.0 μM concentration of the synthetic miR-21 in 1× SSC buffer solution was applied.

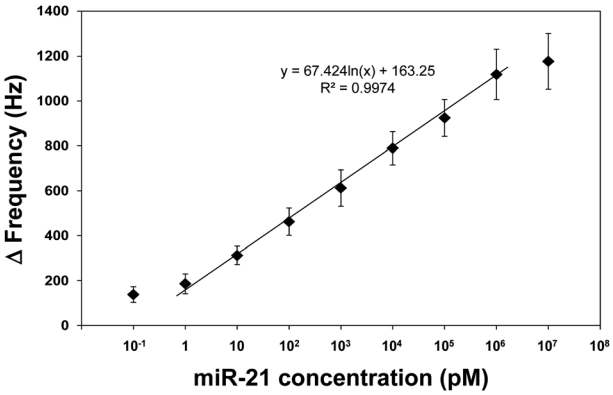

Fig. 5 Changes in resonance frequency of the QCM biosensors according to synthetic miR-21 concentrations in the range (0.1 pM to 10 μM). Dynamic range is at least 7 logarithmic intervals, as observed by the linearity of response of miR-21 at concentration ranging (1.0 pM to 1.0 μM).

over time, as photocatalytic deposition of metallic silver on TiO_2 nanoparticles captured by the sandwich hybridization resulted in significant mass increase at the sensor surface. The solid plot shows the real-time results of decrease in resonance frequency in the hybridization and signal amplification process to detect synthetic miR-21 at a concentration of 1.0 μM on the QCM surface. Also, the dotted line plot shows the result of an increase in resonance resistance in the same experiment. The photocatalytic silver enhancement step can clearly be seen to be the main cause of the decrease of the QCM resonance frequency, and the increase of the resonance resistance.

Dependence of the change in resonance frequency on the synthetic miR-21 concentrations

We investigated the effect of the QCM biosensor response, the resonance frequency change, on the concentration of synthetic miR-21 in a 1× SSC buffer solution (pH 7.0) due to sandwich hybridization and the subsequent photocatalytic silver enhancement processes. Fig. 5 shows the results of the experiments that were carried out in triplicate for each concentration of synthetic miR-21. The (0.1 pM to 10 μM) samples were prepared by 10-fold serial dilution from a 10 μM stock solution of synthetic miR-21, and analyzed based on the assay protocol mentioned above. As the concentration of miR-21 increased, the changes in resonance frequency of the QCM resonator also logarithmically increased. The higher the concentration of miR-21, the greater the sandwich hybridization between the capture probe, the TiO_2-attached detection probe, and the target miR-21; and eventually, the surface concentration of TiO_2 nanoparticles increased. The increase in the surface concentration of these TiO_2 nanoparticles not only causes a mass loading effect in itself, but also significantly increases the frequency change, due to the enlargement of the size of TiO_2 nanoparticles by photocatalytic reduction. Meanwhile, all frequency change values for each concentration shown in Fig. 5 were applied with blank subtraction, to eliminate the influence of environmental factors, such as temperature and viscosity, excluding the effect of mass loading. Unlike general QCM biosensors, in this study, blank subtraction is very important, because the photocatalytic silver enhancement signal amplification process caused a change in viscosity by the addition of $AgNO_3$ solution and a temperature change by UV irradiation. We calculated the limit of detection (LOD) to be as low as 0.87 pM, based on the description based on the following eqn (1) by Shrivastava and Gupta.[33] This is also the recommended estimates in the Clinical and Laboratory Standards Institute (CLSI) guideline EP17.

$$\mathrm{LOD} = \mu_B + 1.645\sigma_B + 1.645\sigma_S \quad (1)$$

where μ_B and σ_B are the mean value and standard deviation of the blank sample measurements and σ_S is the standard deviation of the very low concentration sample measurements. In addition, the correlation coefficient was 0.997, which showed good linearity in the range (1.0 pM to 1.0 μM). These results revealed that the QCM-based miRNA biosensors used in this study had a comparable LOD and correlation coefficient to those of the miRNA sensors that have recently been reported (Table 1).[34–45]

On the other hand, considering the principle of the sandwich hybridization assay of this study, the selectivity of miR-21 detection using the QCM biosensor was excellent. Since the hybridization of oligonucleotides is a highly sequence-specific event, the capture and detection probes designed for miR-21 did not work for other non-complementary miRNAs (miR-124 and miR-155). The response to miR-21, a perfectly matched target, showed a significant signal difference (minimum 17.7-fold), compared to the results for the other two non-complementary miRNAs at the same concentration (1.0 μM). Fig. 6 summarizes the results for the three miRNAs and the blank sample.

Detection of miR-21 in human serum sample

In order to demonstrate the accuracy of our developed QCM biosensor in a real environment, an experiment was performed on miR-21 spike serum samples under the same conditions as in the buffer. In a human serum sample spiked with miR-21 at

Table 1 Comparison of miR-21 detection with the reported methods[a]

Analytical technique	LOD	Linear range	Assay strategy	Ref.
Fluorescence	1.4 pM	1.0 fM to 1.0 pM	Laminar flow-assisted dendritic amplification	34
Fluorescence	2.0 pM	100 pM to 100 nM	TaqMan/duplex-specific nuclease	35
ECL	0.5 fM	1.0 fM to 1.0 nM	Resonance energy transfer	36
SPR	3.0 fM	10 fM to 100 pM	Duplex-specific nuclease	37
Electrochemistry	4.2 fM	5.0 fM to 50 pM	Hairpin/duplex-specific nuclease	38
Fluorescence	2.0 pM	—	Duplex-specific nuclease	39
SPR	47 fM	—	Gold nanoparticles conjugation	40
QCM	0.4 nM	10 nM to 1.0 μM	Avidin nanoparticles conjugation	41
Electrochemistry	29 fM	96 fM to 25 pM	Anti-DNA–RNA hybrid antibodies	42
Fluorescence	0.33 nM	1.0 nM to 50 nM	MnO_2 nanosheet/FAM dyes	43
Fluorescence	0.5 nM	1.0 nM to 50 nM	Molecular beacon/TAMRA dyes	44
SPR	10 aM	100 aM to 100 pM	Gold nanorods conjugation	45
QCM	0.87 pM	1.0 pM–1.0 μM	TiO_2 nanoparticles conjugation	This work

[a] ECL: electrochemiluminescence, QCM: quartz crystal microbalance, SPR: surface plasmon resonance.

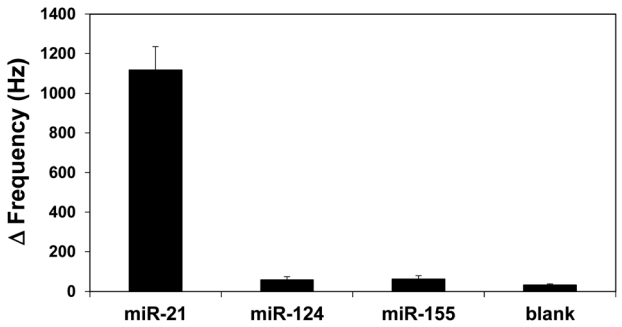

Fig. 6 Selectivity of the QCM biosensors towards miR-21, in comparison with other miRNA (miR-124, miR-155) samples.

a concentration of (1.0 pM to 1.0 μM) generated using a standard spiking method, the changes in resonance frequency were measured in response to the sandwich hybridization event between miR-21 and complementary probes, and subsequent photocatalytic silver enhancement. Three measurements were repeated for each concentration of miR-21, and Table 2 lists the resulting relative standard deviation (RSD) and recovery percentage. The average recovery of miR-21 in serum samples was found to range (97.4 to 105.3)% at each applied concentration level, showing very good miR-21 recovery in all spiked samples. These results showed that a complex and turbid matrix, such as serum, had little effect on the results of QCM detection using this sandwich hybridization and signal amplification. These excellent recovery results also suggest that our developed sensor is potentially useful for analyzing target miRNAs, such as miR-21, in real samples, which makes it an excellent and practical application in cancer clinics and diagnostics.

Table 2 Determination of miRNA-21 concentrations in human serum

Sample	Added (pM)	Found (pM)	Recovery (%)	RSD (%)
1	1	1.047	104.7	5.2
2	10	9.739	97.4	4.8
3	100	105.3	105.3	4.1
4	500	516.8	103.4	4.3
5	1000	974.4	97.4	3.8
6	2500	2467	101.3	3.1
7	5000	5107	102.1	3.5

Conclusions

We successfully implemented a QCM biosensor that applied a sandwich hybridization reaction between a target and probes designed based on the target, and a subsequent TiO_2 photocatalytic silver enhancement reaction, for the detection of target miR-21. The designed QCM biosensor worked selectively for only miR-21, and the LOD was calculated to be as low as 0.87 pM. In addition, the biosensor worked well with complex and turbid matrices, such as human serum, so this approach can be used as a promising alternative for the quantitative detection of miR-21 and other clinically important miRNAs in real samples. The results also show that the biosensor has great potential for real disease diagnosis and various other clinical applications, because of its superior detection performance for miRNA. Along with the development of sensor devices that are capable of simultaneously detecting multiple targets, future work will be focused on improving the performance of the QCM biosensors through reducing the non-specific adsorption by precise sensor surface modification and automated fluid transfer in connection with a UV irradiation device.

Conflicts of interest

There are no conflicts to declare.

Acknowledgements

This work was supported by Soonchunhyang University, and by a National Research Foundation of Korea Grant, funded by the Korean Government (NRF-2019R1F1A1059933).

Notes and references

1 A. P. F. Turner, *Chem. Soc. Rev.*, 2013, **42**, 3184.
2 P. Mehrotra, *Journal of Oral Biology and Craniofacial Research*, 2016, **6**, 153.
3 S. Atay, K. Piskin, F. Yilmaz, C. Cakir, H. Yavuz and A. Denizli, *Anal. Methods*, 2016, **8**, 153.
4 Y. Zhang, F. Lin, Y. Zhang, H. Li, Y. Zeng, H. Hao and S. Yao, *Anal. Sci.*, 2011, **27**, 1229.
5 H. J. Park and S. S. Lee, *Analyst*, 2019, **144**, 6936.
6 H. J. Park and S. S. Lee, *Anal. Sci.*, 2019, **35**, 883.
7 J. Kwak and S. S. Lee, *Nanotechnology*, 2019, **30**, 445502.
8 H. J. Park and S. S. Lee, *Sens. Actuators, B*, 2018, **258**, 836.
9 N. C. Gianneschi, S. T. Nguyen and C. A. Mirkin, *J. Am. Chem. Soc.*, 2005, **127**, 1644.
10 S. W. Thomas, G. D. Joly and T. M. Swager, *Chem. Rev.*, 2007, **107**, 1339.
11 Y. Wang, S. Wang, S. Ge, S. Wang, M. Yan, D. Zang and J. Yu, *Anal. Methods*, 2013, **5**, 1328.
12 O. Makhlynets and I. Korendovych, *Biomolecules*, 2014, **4**, 402.
13 P. Scrimina and L. J. Prins, *Chem. Soc. Rev.*, 2011, **40**, 4488.
14 X. Yang, Y. Tang, S. M. Traynor and F. Li, *J. Am. Chem. Soc.*, 2016, **138**, 14076.
15 M. Vaculovicova, P. Michalek, S. Krizkova, M. Macha and V. Adam, *Anal. Methods*, 2017, **9**, 2375.
16 X. Pei, Z. Xu, J. Zhang, Z. Liu and J. Tian, *Anal. Methods*, 2013, **5**, 3235.
17 E. C. Wang and A. Z. Wang, *Integr. Biol.*, 2014, **6**, 9.
18 H. Zhang, L. Zhang, Y. Ding, W. Zhang, X. Zhang, Y. Shen and F. Yang, *Anal. Methods*, 2016, **8**, 3000.
19 Y.-C. Li, H.-B. Xin, H.-X. Lei, L.-L. Liu, Y.-Z. Li, Y. Zhang and B.-J. Li, *Light: Sci. Appl.*, 2016, **5**, e16176.
20 W. J. Qin and L. Y. L. Yung, *Nucleic Acids Res.*, 2007, **35**, e111.
21 R. Thiruvenkatachari, S. Vigneswaran and I. S. Moon, *Korean J. Chem. Eng.*, 2008, **25**, 64.
22 J. A. Pedraza-Avella, P. Acevedo-Pen and J. E. Pedraza-Rosas, *Catal. Today*, 2008, **133–135**, 611.
23 Y. Zhuo, Y.-Q. Chai, R. Yuan, L. Mao, Y.-L. Yuan and J. Han, *Biosens. Bioelectron.*, 2011, **26**, 3838.
24 M. R. Hoffmann, S. T. Martin, W. Choi and D. W. Bahnemann, *Chem. Rev.*, 1995, **95**, 69.
25 J. V. Tricoli and J. W. Jacobson, *Cancer Res.*, 2007, **67**, 4553.
26 X. Chen, Y. Ba, L. Ma, X. Cai, Y. Yin, K. Wang, J. Guo, Y. Zhang, J. Chen and X. Guo, *Cell Res.*, 2008, **18**, 997.
27 J. Takamizawa, H. Konishi, K. Yanagisawa, S. Tomida, H. Osada, H. Endoh, T. Harano, Y. Yatabe, M. Nagino and Y. Nimura, *Cancer Res.*, 2004, **64**, 3753.
28 K. A. Cissell, S. Shrestha and S. K. Deo, *Anal. Chem.*, 2007, **79**, 4754.
29 Y. H. Feng and C. J. Tsao, *Biomed. Rep.*, 2016, **5**, 395.
30 V. Fulci, S. Chiaretti, M. Goldoni, G. Azzalin, N. Carucci, S. Tavolaro, L. Castellano, A. Magrelli, F. Citarella and M. Messina, *Blood*, 2007, **109**, 4944.
31 H. Muramatsu, M. Kawamura, S. Tanabe and M. Suda, *Anal. Chem. Res.*, 2016, **7**, 23.
32 B. Tumurbaatara, M.-J. Kim, C.-H. Park and C. S. Kim, *Sensing and Bio-Sensing Research*, 2018, **21**, 75.
33 A. Shrivastava and V. B. Gupta, *Chron. Young Sci.*, 2011, **2**, 21.
34 R. Ishihara, K. Hasegawa, K. Hosokawa and M. Maeda, *Anal. Sci.*, 2015, **31**, 573.
35 B.-C. Yin, Y.-Q. Liu and B.-C. Ye, *J. Am. Chem. Soc.*, 2012, **134**, 5064.
36 C. Yang, B. Dou, K. Shi, Y. Chai, Y. Xiang and R. Yuan, *Anal. Chem.*, 2014, **86**, 11913.
37 X. Qiu, X. Liu, W. Zhang, H. Zhang, T. Jiang, D. Fan and Y. Luo, *Anal. Chem.*, 2015, **87**, 6303.
38 Q.-M. Feng, Y.-Z. Shen, M.-X. Li, Z.-L. Zhang, W. Zhao, J.-J. Xu and H.-Y. Chen, *Anal. Chem.*, 2016, **88**, 937.
39 S. Wang, B. Fu, J. Wang, Y. Long, X. Zhang, S. Peng, P. Guo, T. Tian and X. Zhou, *Anal. Chem.*, 2014, **86**, 2925.
40 G. Premaratnea, Z. H. A. Mubaraka, L. Senavirathnab, L. Liub and S. Krishnan, *Sens. Actuators, B*, 2017, **253**, 368.
41 A. Palaniappan, J. A. Cheema, D. Rajwar, G. Ammanath, L. Xiaohu, L. S. Koon, W. Yi, U. H. Yildizd and B. Liedberg, *Analyst*, 2015, **140**, 7912.
42 M. Zouari, S. Campuzano, J. M. Pingarrón and N. Raouafi, *ACS Omega*, 2018, **3**, 8923.
43 T. Xue, W. Liang, Y. Li, Y. Sun, Y. Xiang, Y. Zhang, Z. Dai, Y. Duo, L. Wu, K. Qi, B. N. Shivananju, L. Zhang, X. Cui, H. Zhang and Q. Bao, *Nat. Commun.*, 2019, **10**, 1.
44 W. Ouyang, Z. Liu, G. Zhang, Z. Chen, L. Guo, Z. Lin, B. Qiu and G. Chen, *Anal. Methods*, 2016, **8**, 8492.
45 Q. Liu, J. Fan, C. Zhou, L. Wang, B. Zhao, H. Zhang, B. Liu and C. Tong, *Int. J. Anal. Chem.*, 2018, **2018**, 3625823.